From Waste To Clean Water: A Review Of Activated Carbons Made From Agricultural, Industrial And Municipal Solid Wastes For Dye Adsorption

V. Srinivasulu[1], Anthati Sreenivasulu[2]
[1]*Research Scholar, Assistant Professor of Chemistry, Research Centre in Chemistry, Nagarjuna Government College (Autonomous), Mahatma Gandhi University, Nalgonda*
[2]*Assoc. Professor of Chemistry, Research Centre in Chemistry, Nagarjuna Government College (Autonomous), Mahatma Gandhi University, Nalgonda, Telangana, India*

***Abstract*—Dye-containing wastewater can reduce light in water and harm aquatic life. Activated carbon can remove dyes, but its production and reuse can be costly [1, 2, 3, 4, 5]. This review examines carbons and chars made from agricultural, industrial and municipal wastes. It explains how the starting material, activation method, pore structure and surface chemistry affect dye uptake. It also reviews batch tests, equilibrium models, adsorption rates and thermodynamic calculations. Two tables collect 18 adsorbent–dye entries from the cited literature.**

These entries include both fitted capacities and other reported uptake values, so they do not form a fair performance ranking. The collected values range from about 23 to more than 1000 mg g−1. Selected entries were checked against the abstracts of the cited papers; the remaining values should still be confirmed in the original sources. The main research needs are tests with real wastewater, sound model fitting, clear reuse data, safe handling of spent carbon and complete cost estimates. Waste-derived carbon may offer useful local treatment options, but a low-cost starting material alone does not prove that the final process is cheap or safe.

***Index Terms*—activated carbon; solid waste; dye adsorption; isotherm; kinetics; regeneration; low-cost adsorbent**

I. INTRODUCTION

Dyeing wastewater often contains unfixed dye, salts and other processing chemicals [1, 6]. Small amounts of dye can give water a strong colour. That colour can reduce the light available to aquatic plants. Many dyes also resist biological breakdown because manufacturers design them to remain stable during use [1, 7]. Removing colour matters, but it does not by itself show that the treated water is safe.

Treatment options include coagulation, membranes, biological processes, advanced oxidation and adsorption [6]. Each has limits. Membranes can foul, and biological systems may struggle with stable dyes. Oxidation can produce compounds that need further testing. Adsorption offers a relatively simple way to transfer dyes from water to a solid [5, 7]. It does not necessarily destroy them. The treatment must also deal with the loaded adsorbent and any liquid used to regenerate it.

Activated carbon is a widely used adsorbent, but preparation and regeneration add to its cost. Carbon-rich wastes offer alternative starting materials. Reviews by Crini, Gupta and Suhas, and Rafatullah and colleagues describe many low-cost dye adsorbents [5, 8, 9]. Other reviews explain how crop residues and related wastes can become porous carbons [3, 4, 10]. These studies support further work, not an assumption that every waste-derived carbon will be cheaper than a commercial product.

Comparing the published results is difficult. Studies use different dyes, pH values, carbon doses, temperatures and concentration ranges. Some estimate capacity from a model even when their data do not approach saturation. Others compare models after linear transformations that change the measurement errors [11]. A large reported capacity may therefore reflect the test and fitting method as much as the carbon itself.

This review brings together waste-derived carbons and related chars used for dye removal. It links preparation

conditions to surface properties, adsorption tests and practical limits. It does not report new laboratory measurements.

This article is a narrative review, not a documented systematic review. The literature search used Crossref and OpenAlex. Capacity values in the tables were taken from the cited papers or their abstracts. Search strings, screening counts and a complete extraction record are not presented here, so the tables should be read as a working summary of published reports. Every DOI and capacity value should be checked against the original paper before it is reused. The numbered sources are limited to work published on or before November 2022.

The sections below cover dye properties, waste feedstocks, activation, carbon characterisation and batch testing. They then explain equilibrium, kinetic and thermodynamic models before discussing mechanisms, reported capacities, regeneration, cost and research needs.

II. DYE CLASSES AND WHY THEY MATTER

Dyes can be grouped by their use, such as acid, basic, direct, reactive or disperse dyeing. They can also be grouped by chemical structure, such as azo, triarylmethane, xanthene, anthraquinone or thiazine dyes [7, 8]. For adsorption, charge is especially useful. Basic dyes commonly carry positive charge, while many acid, direct and reactive dyes contain negatively charged sulfonate groups. Charge affects how a dye interacts with a carbon surface, but molecular size, shape and solution pH also matter.

Table 1 lists common test dyes. Researchers often use methylene blue because it is readily available and easy to measure by visible-light absorbance [9, 12]. Crystal violet has medical and laboratory uses, but animal and cell studies have raised concerns about its toxicity [13, 14]. Malachite green also presents risks to aquatic organisms [15, 16]. Some azo dyes can form harmful aromatic amines during breakdown [2]. These risks depend on the dye, its products and the level and route of exposure; they should not be treated as identical for all dyes.

Industrial wastewater can carry more than colour. Salts, treatment chemicals and other pollutants may remain after a dye disappears from view [1, 6]. A useful treatment assessment therefore measures more than the target dye. The choice of extra tests should reflect the actual wastewater source.

Table 1. Dyes most often used in tests on waste-derived carbons. Formulas are for the common salt forms; λ_{max} values are typical figures and should be checked against your own spectrum.

Dye	Charge in water	Chemical family	Formula (salt form)	Typical λ_{max} (nm)	Main concerns
Methylene blue (MB)	Cationic	Thiazine	$C_{16}H_{18}ClN_3S$	≈664	Widely used test dye; harmful at high doses [12]
Crystal violet (CV)	Cationic	Triarylmethane	$C_{25}H_{30}ClN_3$	≈590	Tumours in long-term mouse study; genotoxicity studied [13, 14]
Malachite green (MG)	Cationic	Triarylmethane	$C_{23}H_{25}ClN_2$	≈617	Toxic to aquatic life; residues in farmed fish [15, 16]
Rhodamine B (RhB)	Cationic (zwitterion at high pH)	Xanthene	$C_{28}H_{31}ClN_2O_3$	≈554	Reported as an adulterant in chilli powder [65]
Congo red (CR)	Anionic	Benzidine-based diazo	$C_{32}H_{22}N_6Na_2O_6S_2$	≈497	Can release benzidine-type amines [2]
Methyl orange (MO)	Anionic	Mono-azo	$C_{14}H_{14}N_3NaO_3S$	≈464	Stable azo dye; pH-indicator colour change [7]

A change in colour does not always mean that adsorption has occurred. Methyl orange changes colour with pH. Congo red can change its spectrum and aggregate under acidic conditions. Rhodamine B also changes chemical form as solution conditions change [7, 11]. Measure spectra and prepare calibration solutions under conditions that match the samples. If a method adjusts pH before measurement,

first check that the adjustment does not cause dye loss or alter sample recovery.

UV–visible spectroscopy links absorbance to dye concentration through a calibration curve. Use samples within the validated concentration range and dilute stronger samples when needed. Fine carbon particles can scatter light. Filters can also retain dye. Include a dye-only control, a carbon blank and a filter-recovery check to separate these effects from adsorption [11]. Report the separation method and calibration conditions so that another laboratory can repeat the work.

Pore access depends on molecular shape as well as charge. Methylene blue is relatively flat, while crystal violet and malachite green have bulkier structures. Congo red is larger and can form aggregates. A carbon that removes methylene blue well may therefore perform poorly with a larger dye [7, 9]. One test dye cannot represent every industrial colourant.

III. SOLID WASTES AS CARBON PRECURSORS

A useful carbon precursor combines carbon content, reliable supply and manageable processing costs. Lignocellulosic wastes contain cellulose, hemicellulose and lignin. These components break down differently during heating, which affects carbon yield and pore formation [3, 10].

Table 2 groups the waste sources and notes practical concerns. A low ash content can help in many applications, but mineral matter can also affect surface chemistry and adsorption; its role needs measurement rather than a blanket judgement.

Table 2. Kinds of solid waste used to make dye adsorbents, with examples from the cited literature.

Source group	Typical examples	Points to watch	Example references
Field crop residues	Stalks, husks, straw, cobs (mustard stalk, corn cob, corn husk, rice husk, sorghum)	Seasonal supply; silica-rich ash in husks	[66, 67, 44, 18, 36]
Fruit and food waste	Peels, seeds, shells, stones (pomegranate peel, orange and lemon peel, horse gram seed, date stones)	Wet when fresh; sugars and oils; needs quick drying	[23, 22, 68, 24]
Wood and forest residue	Sawdust, bark, wood chips, bamboo waste	Lignin-rich; good for strong carbons	[38, 33]
Agro-industrial residues	Coir pith, bagasse, oil palm fruit bunch, palm kernel shell	Large central supply at mills	[19, 34, 69]
Industrial wastes	Bagasse fly ash, red mud, leather shavings	Possible metals or other contaminants; leaching tests needed	[25, 26]
Municipal and household waste	Sewage sludge, spent tea leaves, temple flower waste	Variable make-up; hygiene and pre-sorting	[27, 70, 28]

Agricultural residues appear often in this literature because they offer many possible carbon sources. Kadirvelu and colleagues tested carbons from several agricultural wastes for dye and metal removal [17]. Other studies used coir pith for Congo red and rice husk or corncob for crystal violet [18, 19, 20]. These examples show that several feedstocks can work, but local supply and existing uses still affect their value.

Food and fruit wastes provide another group of precursors. Earlier work tested raw orange peel as an adsorbent [21], while later studies converted orange and lemon peel into activated carbon [22]. Other examples include pomegranate peel and horse gram seed [23, 24]. Raw peel, biochar and activated carbon are different materials. Their names and preparation steps should remain clear in any comparison.

Industrial and municipal wastes need particular care. Studies have tested bagasse fly ash and red mud for Congo red removal [25, 26], but neither material should automatically be called activated carbon. Sewage sludge can serve as a precursor for activated carbon [27]. Such feedstocks may contain metals or other contaminants, so tests should examine what the final adsorbent releases into water. Temple flower waste offers another possible resource, although a waste-management reference alone does not establish adsorption performance [28].

Preparation begins before the furnace. Wash the feedstock to remove loose dirt and soluble matter, then dry it to a defined basis. Residual water changes the effective activator-to-solid ratio. Grinding and sieving improve consistency. Moisture, volatile matter, ash and fixed carbon help describe the starting material [3, 4]. Record storage conditions too, since biological decay can change wet residues before processing.

Feedstock selection also needs practical checks. Record when the waste is available, how much can be collected and how far it must travel. Identify competing uses, such as fuel or animal feed. Check likely contaminants and the effort needed for drying and milling. These factors may matter more than a small difference in laboratory uptake [4, 5].

Biochar usually refers to a biomass-derived solid made under oxygen-limited heating. Activated carbon undergoes treatment designed to develop accessible pores; a biochar can also undergo activation [10, 29]. The terms can overlap in published work. This review retains each source's material label, but that label does not prove that two materials have the same structure or treatment history.

IV. MAKING THE CARBON: ACTIVATION ROUTES

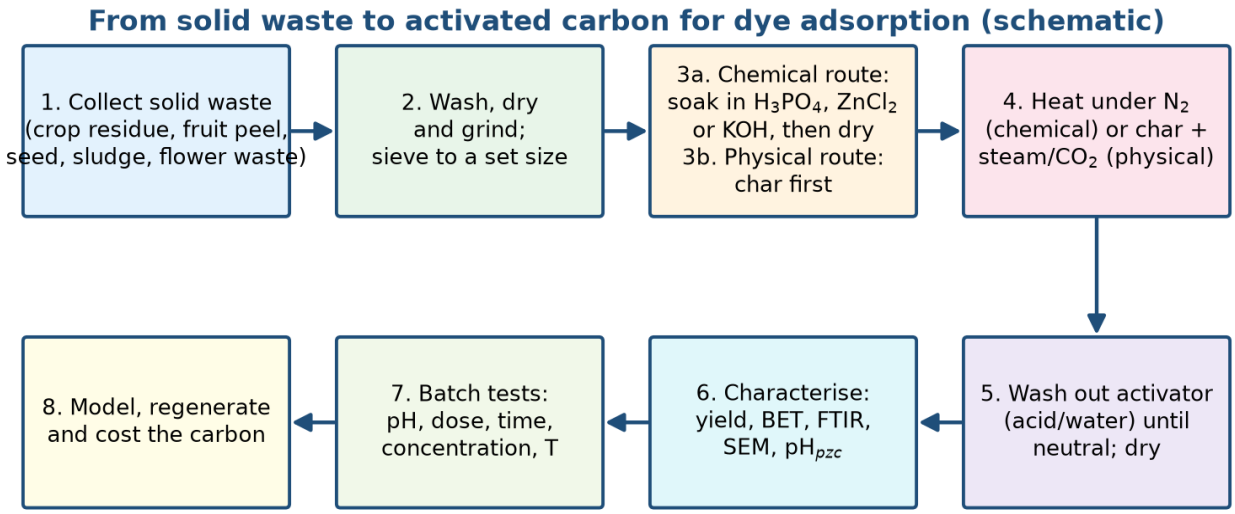


Figure 1. Typical steps from solid waste to a tested activated carbon (schematic). Exact temperatures, ratios and times vary between studies; take them from each paper's methods.

Figure 1 outlines the main preparation steps. Physical activation usually begins with carbonisation under an inert atmosphere. Steam or carbon dioxide then reacts with part of the char and develops pores. Chemical activation uses an agent such as phosphoric acid, zinc chloride or potassium hydroxide before or during heat treatment [3, 4, 10, 30]. The best route depends on the precursor and the desired material. Chemical activation can lower the required temperature in some systems, but it also creates washing and chemical-recovery needs.

4.1 Phosphoric acid (H_3PO_4)

Phosphoric acid is widely used with lignocellulosic feedstocks. It promotes dehydration and structural changes that help preserve a porous solid during heating [31]. Washing removes soluble residues. The final carbon may contain acidic oxygen- and phosphorus-bearing groups and a mix of micro- and mesopores. These properties can support cationic dye uptake, but performance still depends on pH and pore access. Corncob-derived carbon is one published example [20].

4.2 Zinc chloride ($ZnCl_2$)

Zinc chloride promotes dehydration and pore development during heating [30, 32]. Studies have used it with sawdust and bagasse [33, 34]. The benefit comes with a clear responsibility: remove residual zinc and treat the zinc-bearing wash water. A porous

carbon is not suitable for water treatment if it releases unacceptable contaminants. Report the washing process and test the final material for leaching [32].

4.3 Potassium hydroxide (KOH)

KOH activation can create a highly porous carbon. Its reactions at high temperature involve potassium-containing compounds and, under suitable conditions, metallic potassium that enters the carbon structure [35].

Sorghum-waste carbon is one published example of this route [36]. High surface area is useful only when the dye can reach that surface. KOH use, corrosion, carbon yield and wash-water treatment also affect the process.

4.4 Other routes

Other approaches suit different feedstocks. Hydrothermal carbonisation treats wet biomass in hot, pressurised water and produces hydrochar [37]. It does not automatically produce activated carbon. Microwave heating can reduce treatment time in some published processes [4, 10]. Adding iron oxide can aid magnetic separation, but it adds processing steps and may change accessible pore space [38].

4.5 Settings that change the result

Four preparation variables need clear reporting: activator-to-dry-precursor ratio, temperature, holding time and heating rate. Increasing treatment severity may open pores, but excessive treatment can widen pores, consume carbon and lower yield [4, 30]. The trend varies by feedstock, so those four settings should be stated with the yield and a pore-structure measurement.

Report dry-basis yield alongside adsorption capacity. A high-capacity carbon may still require too much feedstock or energy if little solid survives preparation. For a washed and dried product, use:

Yield (%) = 100 × (mass of washed, dried carbon) / (mass of dry precursor) (1)

Post-activation washing removes soluble acid, alkali and salts. The washing method should match the activation chemistry [32, 35]. A near-neutral final wash is useful information, but it does not prove that all residues are gone. Measure relevant species, such as zinc, phosphate or potassium, when needed. Record wash-water volume and manage the resulting liquid safely. Heating and concentrated-chemical steps also require appropriate laboratory controls.

Table 3. Plain comparison of the main activation routes (qualitative, drawn from the cited reviews).

Route	How it works	Typical surface	Main advantages	Main drawbacks	Refs
Physical (steam/CO2)	Char first, then partial gasification	Mostly micropores	No added chemical activator; off-gas and wash streams still need assessment	Two steps; high temperature; lower yield	[3, 10]
H3PO4	Acid attack, cross-linking, phosphate bridges	Micro- and mesopores; acidic groups	Lower temperature; good yield; suits cationic dyes	Acid recovery; P in wash water	[31]
ZnCl2	Dehydration and templating	Micro- and mesopores	High yield; well-developed pores	Zinc removal and disposal	[30, 32]
KOH	Redox reactions and K intercalation	Very high area; mostly micropores	Can produce very high surface area	Corrosive; large KOH use; lower yield	[35]

V. DESCRIBING THE CARBON

Removal percentage alone says little about why a carbon works. Surface area and pore-size tests describe accessible space. FTIR identifies broad groups of surface bonds. Electron microscopy shows texture, while surface-charge measurements help explain pH effects. Table 4 summarises these methods. Use them together rather than treating one result as proof of performance.

5.1 BET surface area and pore size

The Brunauer–Emmett–Teller method estimates surface area from gas adsorption. Nitrogen at 77 K is common, but the chosen pressure range and model assumptions matter [39, 40]. Dyes cannot enter every pore that a small gas molecule can reach. A material with suitable transport pores and accessible adsorption sites may therefore outperform one with a larger reported BET area. Follow IUPAC guidance when analysing and reporting pore structure [40].

5.2 FTIR

FTIR spectra help identify hydroxyl, carbonyl and other surface groups. Phosphoric-acid treatment can also leave phosphorus-containing groups [10, 41]. A change in a band after adsorption may support an interaction, but overlapping signals, moisture and measurement conditions can also change spectra. Compare consistent preparations and use other evidence before assigning a mechanism.

5.3 SEM and related tests

SEM images show cracks, external texture and larger openings. They do not directly establish micropore volume. EDX can detect elements such as zinc or phosphorus in the measured region, but it does not replace a leaching test. A smoother image after adsorption is not enough to prove that dye filled the pores [10].

5.4 Point of zero charge and Boehm titration

The point of zero charge, pHpzc, describes the pH at which the measured net surface charge is zero. Under the stated test conditions, the surface often becomes more positive below this value and more negative above it [42]. This helps interpret adsorption, although it does not predict every interaction. Boehm titration estimates classes of acidic and basic surface groups [43]. Report the method and solution conditions, since different procedures can give different results.

5.5 Other useful tests

Other methods answer more specific questions. X-ray diffraction helps identify structural order and crystalline mineral phases. Thermogravimetric analysis tracks mass loss during heating. Elemental analysis measures bulk composition, while XPS examines near-surface chemical states [10, 41]. Choose methods that test the proposed explanation rather than adding measurements without a clear purpose.

A useful reporting set includes yield, ash, gas-adsorption data, pore-size analysis, FTIR, SEM and pHpzc. This is a practical proposal, not a universal publication rule. Contaminated feedstocks also need appropriate leaching tests. Provide enough detail for readers to connect preparation, surface properties and adsorption behaviour.

Table 4. Common characterisation tests and what they reveal about a dye adsorbent.

Test	What it measures	Why it matters for dyes	Refs
N2 adsorption (BET, BJH/DFT)	Surface area, pore volume, pore-size spread	Dye size versus pore size controls access	[39, 40]
FTIR	Surface functional groups	Points to H-bonding, electrostatic and n–π sites	[41]
SEM / SEM-EDX	Texture, pore openings, element map	Detects elements locally; does not quantify leaching	[10]
pHpzc (drift or mass titration)	pH of zero net surface charge	Helps interpret pH-dependent charge; does not establish the optimum alone	[42]
Boehm titration	Carboxylic, lactonic, phenolic and basic groups	Explains charge and binding sites	[43]
Iodine / MB number, yield, ash	Micropore and mesopore indices; process efficiency	Quick screening and cost basis	[4]

VI. BATCH VARIABLES

A batch test combines a known carbon mass with a known volume of dye solution. After mixing and separation, the remaining dye concentration gives the uptake by mass balance. The calculation assumes that the measured loss comes from adsorption rather than precipitation, decomposition or handling losses [11]:

$$q_e = (C_0 - C_e)\, V / m \quad (2)$$

$$\text{Removal}\ (\%) = 100\,(C_0 - C_e) / C_0 \quad (3)$$

C_0 and C_e are the starting and equilibrium concentrations in mg L^{-1}. V is solution volume in litres, and m is dry adsorbent mass in grams. Correct the mass balance if repeated sampling changes the solution volume or removes a substantial amount of dye. The following variables affect the result.

6.1 pH

pH affects both the carbon surface and the dye. A surface above its pHpzc often favours attraction of cationic dyes; below pHpzc, it may favour anionic dyes [7, 11]. Lemon-wood carbon provides one published example of pH-sensitive uptake [38]. These are trends, not rules.

Non-electrostatic interactions and changes in the dye can also control the outcome.

Measured pH before and after the contact because the carbon can change it. Use a pH range in which the dye remains suitable for the measurement method. At strongly acidic conditions, for example, Congo red can change colour or aggregate. Include dye-only controls so that these changes do not appear as adsorption [11].

6.2 Adsorbent dose

Adding more carbon often increases the fraction of dye removed because more sites become available. Uptake per gram may fall at the same time, since the available dye spreads across more carbon. Report both percentage removal and mass-normalised uptake. An optimum dose applies only to the tested concentration, volume and treatment target.

6.3 Contact time

Uptake often starts quickly and then slows as the concentration difference falls and transport into pores becomes important. The time needed depends on the dye, particle size, pore structure and mixing. Continue the test until the data support a stable endpoint. Do not assign equilibrium simply because an earlier study used the same contact time.

6.4 Starting concentration

A higher starting concentration can increase uptake per gram, while the percentage removed may fall. The trend is system-specific, not inevitable. Use a concentration range wide enough to test the chosen isotherm and, where possible, approach a plateau [11].

6.5 Temperature

Temperature effects differ between systems. The corn-husk study reports Langmuir capacities of 462.96, 546.45 and 662.25 mg g^{-1} at 298, 308 and 318 K, respectively [44]. Its abstract also states that Freundlich gave the best fit, so the Langmuir values need that qualification. Guava-leaf carbon provides a reported example of exothermic Congo red uptake [45]. Do not assume the direction of the effect before testing it.

6.6 Other factors

Background salts, competing dyes and other wastewater components can alter adsorption. They may compete for sites, screen charge or change dye aggregation. Particle size, mixing and liquid volume also affect the test [7]. Record these conditions and include a realistic water matrix when practical.

6.7 Good laboratory practice in batch tests

Use independent repeat tests and report their spread. Include dye-only controls to check for losses to containers, filters, light or chemical change. Measure final pH and keep mixing, vessel geometry and separation methods consistent. Record stock-solution preparation and storage [11]. These checks make a small data set more useful than a larger one with uncertain recovery.

Plan sampling around the question. Isotherms need enough concentrations to define their shape and constrain fitted parameters. Kinetic tests need early samples as well as a clear endpoint. Temperature studies need enough points and a suitable range to assess uncertainty. Suggested point counts are planning aids, not universal proof that a model is valid.

VII. EQUILIBRIUM ISOTHERMS

An equilibrium isotherm relates q_e to C_e at a fixed temperature. It summarises uptake across a concentration range. Several models can fit the same data, so fitting alone does not establish a molecular mechanism [46, 47, 48].

7.1 Langmuir

The Langmuir model assumes equivalent sites, single-layer occupancy and no lateral interaction between adsorbed molecules [49]. A common solution-phase form is:

$$q_e = q_m K_L C_e / (1 + K_L C_e) \quad (4)$$

q_m is the fitted limiting capacity in mg g−1, and K_L has units of L mg−1 in this concentration form. The often-used separation factor is $R_L = 1/(1 + K_L C_0)$ [46]. With positive K_L and C_0, R_L lies between zero and one by construction; this is not independent proof of useful treatment or thermodynamic favourability. If the data do not approach a plateau, q_m may be poorly constrained and far above measured uptake.

7.2 Freundlich

The empirical Freundlich equation describes a power-law relation over the fitted concentration range [46, 48]:

$$q_e = K_F C_{e1/n} \quad (5)$$

K_F depends on the chosen concentration and uptake units. The exponent 1/n controls curvature; values between zero and one describe a curve that rises less steeply as concentration increases. A fit does not directly measure surface heterogeneity. The equation has no finite plateau and cannot supply a maximum capacity.

7.3 Temkin

The Temkin model describes a decline in adsorption energy with increasing surface coverage under its assumptions [46]. For an empirical concentration-based fit, write:

$$q_e = B_T \ln (A_T C_e) \quad (6)$$

B_T must have the same uptake units as q_e, and $A_T C_e$ must be dimensionless. If C_e is in mg L−1, A_T has reciprocal concentration units. Do not identify B_T as an energy in J mol−1 when q_e is in mg g−1. Converting a fitted coefficient to an adsorption-energy parameter requires a consistent coverage and unit definition. Use this model within a range where its shape is appropriate.

7.4 Dubinin–Radushkevich

The Dubinin–Radushkevich model originated in pore-filling descriptions. Its general mathematical form is:

$$q_e = q_{DR} \exp(-\beta \varepsilon^2), \quad E = (2\beta)^{-1/2} \quad (7)$$

Here ε is an adsorption potential with energy-per-mole units, and β must use matching units. The common solution expression $\varepsilon = RT \ln (1 + 1/C_e)$ is not dimensionally meaningful when C_e carries concentration units [50]. This revision therefore does not present that expression as a valid recipe. A justified standard-state or activity-based formulation is needed. Fixed energy cut-offs should not serve as proof of physical adsorption or chemisorption.

7.5 Fitting and error analysis

Fit the original model equations rather than relying only on linearised plots. Transformations change how measurement errors influence the result [11, 51]. Compare residuals in the original uptake units, report parameter uncertainty and explain any weighting. RMSE gives a direct error summary. A statistically meaningful chi-square calculation needs measurement variances, not simply division by calculated uptake.

$$\text{RMSE} = [\Sigma (q_{e,e} - q_{e,cal})^2/N]^{1/2}; \quad \chi^2 = \Sigma[(q_{e,e} - q_{e,cal})^2/\sigma_i^2] \quad (8)$$

N is the number of observations, and σ_i is the estimated standard deviation for observation i. An uptake-weighted error sum is not automatically a statistical chi-square test. When models have different parameter counts, use a suitable complexity-aware criterion and check whether the parameters are identifiable.

7.6 Choosing and reporting a model

Start with a plot of measured q_e against C_e. Look for a plateau, changes in curvature and unusual points. Fit plausible models and examine their residuals. Add a more flexible model, such as Sips or Redlich–Peterson, only when the data justify its extra parameter [46, 47]. Report parameter estimates with uncertainty. A high R^2 from a transformed plot can hide a poor fit in the original units. Keep temperatures, concentration ranges and fitting procedures visible when comparing q_m values. A good fit is a description of the data, not proof that all model assumptions hold [11, 51].

VIII. KINETICS

Kinetic models describe how uptake changes with time. Pseudo-first-order and pseudo-second-order models are common examples [52, 53].

$$\text{PFO: } q_t = q_e [1 - e^{(-k_1 t)}] \quad (9)$$

$$\text{PSO: } q_t = k_2 q_e^2 t / (1 + k_2 q_e t) \quad (10)$$

q_t is uptake at time t. With time in minutes and uptake in mg g−1, k_1 has units of min−1 and k_2 has units of g mg−1 min−1. A better PSO fit does not prove chemisorption. Sampling near equilibrium and the fitting method can affect which model appears to perform best [11, 54]. Treat the model as a time-course

description unless separate evidence supports a mechanism.

The Elovich equation provides another empirical description for some systems [55]. Researchers also use the Weber–Morris relation to examine uptake against the square root of time [56]:

$q_t = k_{id}\, t_{1/2} + C$ (11)

A linear region suggests that diffusion-related behaviour may matter.

A line near the origin can be consistent with an intraparticle-diffusion contribution, but it does not prove that pore diffusion is the only rate limit. Multiple regions can arise as transport and concentration change.

The intercept is an empirical fitting term; it is not a direct measurement of boundary-layer thickness [11, 56].

Collect early samples before most uptake has finished, then continue to equilibrium. Adjust the schedule after a preliminary run rather than using the same times for every carbon. Test mixing effects when external mass transfer may matter. Fit PFO and PSO in their original forms and report uncertainty in both rate constants and equilibrium uptake [11, 54].

IX. THERMODYNAMICS

Equilibrium measurements across temperature can support thermodynamic estimates if the chosen equilibrium constant and standard states are valid [57]:

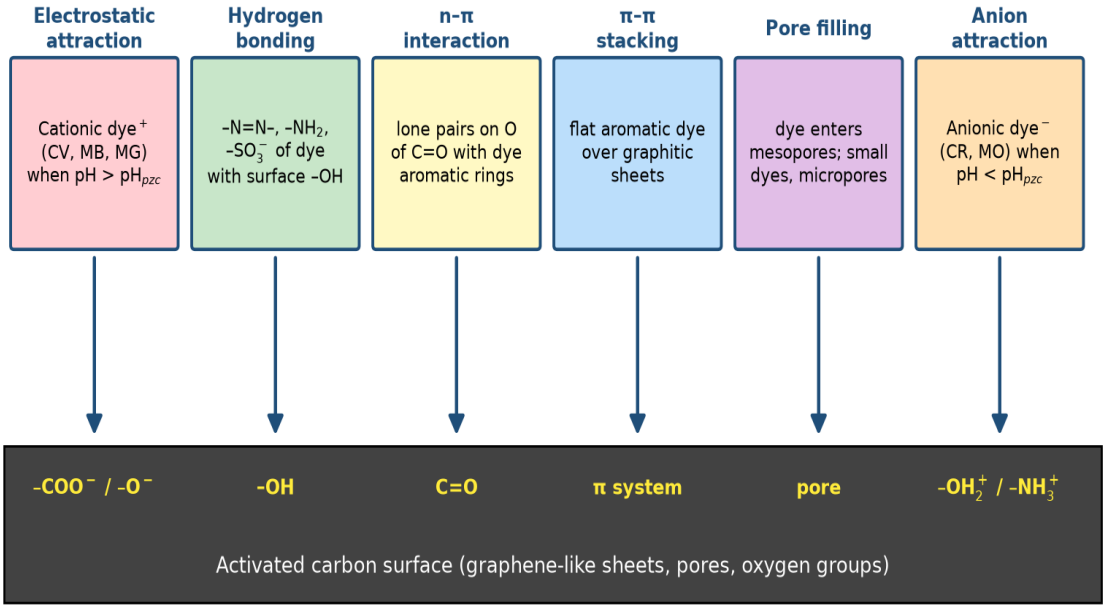
$\Delta G^\circ = -RT \ln K_c$ (12)

$\ln K_c = \Delta S^\circ/R - \Delta H^\circ/(RT)$ (13)

Kc must be a dimensionless equilibrium constant. A dimensional KL or qe/Ce cannot enter the logarithm without a justified thermodynamic definition [11, 57]. A negative ΔG° indicates a standard-state preference, not the direction of every actual experiment. The direction depends on composition through $\Delta G = \Delta G^\circ + RT \ln Q$. The sign of ΔH° describes the fitted overall enthalpy change within the stated range.

Adsorption from water includes changes in the dye, the carbon and surrounding water. Desolvation and water release can contribute to the measured enthalpy and entropy. Their signs alone do not prove a specific molecular sequence. State the equilibrium definition, temperature range, assumptions and uncertainty. A straight van't Hoff fit also assumes that the relevant thermodynamic parameters change little over that range [57].

X. HOW DYES STICK: MECHANISMS



Several routes usually act together; the balance shifts with pH, ionic strength and the carbon's surface chemistry (schematic, not to scale)

Figure 2. Main ways a dye molecule can bind to an activated carbon surface (schematic).

Figure 2 shows possible contributions to dye uptake. Several can act together, and their importance changes with the dye, surface and solution [7].

The schematic presents hypotheses, not direct observations.

- Electrostatic attraction. Opposite charges on dye and carbon can favour uptake. Compare this explanation with measured p^{H}_{pzc}, solution pH and the dye's charge state [7].
- Hydrogen bonding. Surface groups can interact with suitable donor or acceptor groups on a dye. The presence of these groups alone does not show that hydrogen bonding dominates [7].
- n–π interactions. Lone-pair-bearing surface groups may interact with aromatic dye systems. This remains a proposed contribution unless experiments support it [7].
- π–π interactions. Aromatic regions of a dye can interact with aromatic carbon surfaces. Such interactions may help explain uptake when electrostatic attraction is weak [7].
- Pore filling. Molecules can occupy pores that they can access. Pore width, connectivity, surface chemistry and dye aggregation all influence that access [7, 40].

Build a mechanism from several independent observations. Combine pH and salt tests with surface-charge measurements, spectra and desorption data. A single FTIR shift or model fit is weak evidence [7, 11]. The crystal-violet–montmorillonite study offers an example of a more detailed surface-interaction approach, but clay is not activated carbon [58].

Salt tests need careful interpretation. Added ions can screen charge, compete for sites or change dye aggregation. Desorption can also reflect solubility and pore access as well as binding strength. Look for agreement across methods and discuss alternative explanations. Do not arrange the methods into fixed evidence ranking that applies to every adsorbent [7, 11].

XI. WHAT CAPACITIES HAVE BEEN REPORTED?

Tables 5 and 6 collect 18 adsorbent–dye entries from the cited literature. They combine fitted limiting capacities and other reported uptake values. They also cover different pH values, temperatures, doses and concentration ranges. Figure 5 displays these numbers, not a controlled ranking. Selected checks confirmed the corn-husk values [44] and the 1111.1 mg g−1 locust-bean value [59] against the abstracts of those papers. The other entries should still be confirmed in the original sources.

Table 5. Reported uptake values for cationic dyes, taken from the cited papers. The capacity column includes different types of uptake estimate, so the rows are not a ranking. Check each value in the original paper before you reuse it.

Dye	Waste precursor	Carbon type (as named by authors)	Reported uptake (mg g−1)	Condition / model stated	Ref.
MB	Corn cob	Activated carbon	333	Langmuir fit	[67]
MB	Corn husk	$ZnCl_2$-activated carbon	462.96 (298 K); 546.45 (308 K); 662.25 (318 K)	Langmuir q_m; Freundlich fitted best	[44]
MB	Sorghum waste	KOH-activated porous carbon	98.1	Adsorption amount reported	[36]
MB	Mustard stalk	Activated carbon	212.76	Langmuir	[66]
MB	Horse gram seed	Activated carbon	312.5	Maximum capacity	[24]
CV	Palm kernel shell	Biochar	24.45	Langmuir	[69]
CV	Pomegranate peel	Activated carbon	23.26 (27 °C); 76.92 (32 °C)	Langmuir	[23]
CV	Lemon wood	Activated carbon	23.6	D–R described equilibrium	[38]
CV	Cocoa leaves	$ZnCl_2$-activated biochar	253.3	Liu model	[71]

CV	Corncob	H_3PO_4-activated carbon	320.0	Langmuir	[20]
RhB	Bamboo	Activated carbon	111.11	Langmuir, 300 K	[72]
RhB	Okra waste	Activated carbon	321.50	Langmuir, 25 °C	[73]
RhB	Locust bean pod	Functionalised activated carbon	1111.1	Monolayer capacity	[59]

MB = methylene blue; CV = crystal violet; RhB = rhodamine B. The corn-husk values [44] and locust-bean value [59] were confirmed in accessible source text during revision. Other entries remain provisional. Reported maxima, model estimates and measured uptake are not interchangeable.

Table 6. Reported uptake values for anionic dyes, taken from the cited papers. Different conditions and uptake definitions limit comparison, so the rows are not a ranking.

Dye	Waste precursor	Carbon type (as named by authors)	Reported uptake (mg g−1)	Condition / model stated	Ref.
CR	Guava leaf	Activated carbon	47.62	Exothermic uptake	[45]
MO	Finger citron residue	Activated carbon	934.58	Equilibrium capacity	[74]
MO	Orange and lemon peel	Activated carbon	33	Langmuir	[22]
MO	Lignin	$ZnCl_2$-activated carbon	300	Maximum capacity	[75]
AB25	Wild date stones	Activated carbon	181.59	Langmuir	[68]

CR = Congo red; MO = methyl orange; AB25 = Acid Blue 25. Check the original study for each value, its uncertainty, its definition and the test conditions before using it in a comparison.

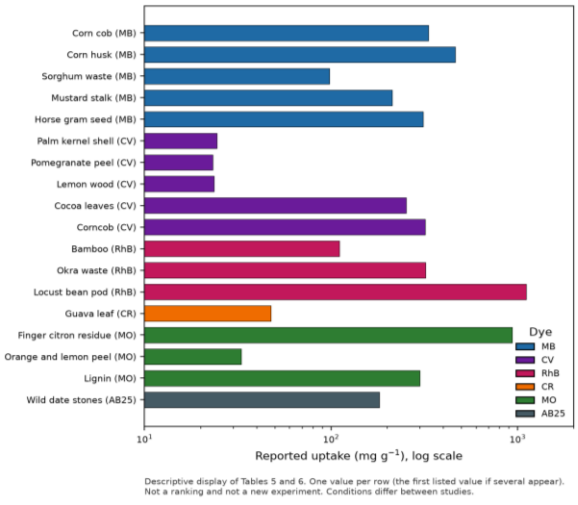


Figure 3. Descriptive display of the uptake values in Tables 5 and 6. The plot uses one value per entry and the first listed value where several appear. The logarithmic scale does not make the studies comparable. This is not a performance ranking or a new experiment.

The retained values span a wide range, from 23.26 mg g−1 for pomegranate-peel carbon at 27 °C [23] to 1111.1 mg g−1 for functionalised locust-bean-pod carbon [59]. The latter value appears in the accessible source abstract. The lower value remains a retained draft entry pending checking. This selected set cannot establish that one activation route is generally best. Different dyes, feedstocks and conditions confound that comparison.

Keep measured uptake separate from model limits. A fitted Langmuir qm can exceed the highest measured uptake in the same study if the experiment never reached a plateau. Tran and co-workers discuss this and related reporting problems [11]. Do not treat a model limit as a measured result.

Compare carbons at similar conditions and with matching uptake definitions. Check concentration range, saturation, repeatability and fitting uncertainty. Surface-area-normalised uptake can add context, but nitrogen-accessible BET area is not necessarily dye-accessible area [11, 40, 51]. An extra normalisation cannot remove differences in dye chemistry or test design.

XII. REGENERATION, REUSE AND DISPOSAL

Regeneration aims to restore useful adsorption after dye loading. Methods include heat treatment and chemical washing [60, 61]. The suitable method depends on the dye and carbon. Acid can promote

desorption of some cationic dyes, while alkali may help with some anionic systems. Percentage removal after a reuse cycle is not the same as retained capacity, because the carbon mass, the eluent and the loading conditions all matter. Purkait and colleagues studied regeneration after Congo red adsorption [61]. Salvador and co-workers reviewed thermal regeneration of carbonaceous adsorbents [60].

Regeneration produces another waste stream: a smaller volume of liquid with concentrated dye and possibly treatment chemicals. Record its handling. Spent carbon may require controlled treatment or disposal. Burning, solidification or incorporation into another material needs an assessment of emissions, leaching and applicable rules, not an assumption of safety [60, 61].

Use the same loading conditions in each reuse cycle. Report uptake, removal percentage, recovered carbon mass, eluent strength and volume, and treatment time. Correct for carbon loss where appropriate. Several cycles help reveal trends, but no single cycle count proves industrial durability. Explain whether a decline may reflect lost material, changed surface chemistry or incomplete regeneration [60, 61].

XIII. GAPS AND OUTLOOK

The studies discussed here point to six practical reporting and research needs. Table 8 summarises them. These are priorities for stronger evidence, not claims that every paper lacks the same information.

Table 7. Research and reporting needs for waste-derived carbons used in dye removal.

Gap	Why it matters	Suggested step
Synthetic single-dye tests only	Real effluent has salts, surfactants and many dyes	Test at least one real or simulated mixed effluent
Linear fitting and R2 only	Constants and model choice can be wrong [11, 51]	Use non-linear fitting with at least one error function
Mechanism claimed from PSO fit	PSO fit does not prove chemisorption [54]	Combine pH, ionic strength, FTIR and desorption evidence
Thermodynamics with unit errors	Wrong $\Delta G°$ and $\Delta S°$ [57]	Use a dimensionless K_c and state the conversion
Few reuse and disposal data	Hides true cost and risk [60]	Run and justify repeated cycles; report uptake, carbon loss and fate of wastes
Limited cost or scale-up evidence	'Low-cost' claim is untested [62]	Give a simple cost sheet and run a fixed-bed column test

Several directions deserve testing. Columns provide breakthrough data under flow [27]. Mixing precursors may change surface chemistry, but any benefit needs a controlled comparison. Local residues may reduce transport distance, although their availability needs documentation. Published marigold-straw carbon and custard-apple-shell carbon studies show possible preparation routes [63, 64]. The custard-apple study concerns energy storage, so it does not establish dye-removal performance.

Better reporting can be as useful as a new precursor. Share preparation conditions, yield, pore data, pHpzc, raw equilibrium and kinetic results, uncertainty and fitting procedures. Add properly defined thermodynamics only where the data support it. Report repeated reuse tests and, where possible, a realistic water matrix. These data help others reproduce the work and test its interpretation.

Batch tests estimate uptake under mixed conditions. A packed column also tests flow, bed use and breakthrough. It can reveal clogging, channel formation and limits that a flask test misses. The cited sewage-sludge-carbon study includes both batch and fixed-bed work [27]. Column results need bed dimensions, packing, particle size, flow rate and inlet and outlet concentrations to support useful scale-up.

Real dyehouse water can contain several dyes, salts, surfactants and other processing chemicals. These components can compete, alter surface interactions or block access to sites [1, 7]. A single-dye result in clean water is an important first step, not a field-performance guarantee. Measure the actual effluent and define the treatment target before judging success.

Local projects can connect waste collection with water treatment, but the supply chain needs evidence. A proposed local case study should document the waste source, seasonal supply, transport distance and wastewater composition. This review does not report a field survey of local markets, temples or dyeing units, and it does not treat such a setting as an established case.

The following questions provide a practical agenda:

- Does a given waste carbon keep its capacity in real dyehouse water, with salts and surfactants present?
- How many reuse cycles can it survive, and what happens to the concentrated eluate?
- Which surface groups actually bind the dye, as shown by spectra before and after uptake, not just by model fits?
- How does cost per gram of dye removed compare with commercial carbon, once energy, chemicals and labour are counted?
- Can a small fixed-bed column built from the carbon treat a real effluent stream for a useful number of bed volumes?
- Is the spent carbon safe to burn, bury or reuse, as judged by a standard leaching test?

XIV. CONCLUSIONS

Waste-derived carbons can adsorb several classes of dye from water. The feedstock and activation route affect yield, pores and surface chemistry. Dye charge, pH and access to pores then influence uptake [3, 4, 7, 10]. The retained capacity tables show a wide range, but their mixed conditions and uptake definitions prevent a fair ranking.

A high fitted capacity is not enough to establish practical value. Real-water tests, uncertainty, reuse, contaminant release and full process costs are also needed.

A useful study begins with a well-described local feedstock and a repeatable preparation method. It then links material properties to controlled adsorption tests and reports the raw data. Flow tests and safe management of regeneration waste bring the work closer to use [11, 27, 60, 62]. A modest, reproducible result with clear limits offers more value than an impressive number without enough evidence.

REFERENCES

[1] B. Lellis, C. Z. Fávaro-Polonio, J. A. Pamphile, and J. C. Polonio, "Effects of textile dyes on health and the environment and bioremediation potential of living organisms," *Biotechnology Research and Innovation*, vol. 3, no. 2, pp. 275–290, 2019, doi: 10.1016/j.biori.2019.09.001.

[2] K. T. Chung, "Azo dyes and human health: A review," *Journal of Environmental Science and Health, Part C*, vol. 34, no. 4, pp. 233–261, 2016, doi: 10.1080/10590501.2016.1236602.

[3] O. Ioannidou and A. Zabaniotou, "Agricultural residues as precursors for activated carbon production—A review," *Renewable and Sustainable Energy Reviews*, vol. 11, no. 9, pp. 1966–2005, 2007, doi: 10.1016/j.rser.2006.03.013.

[4] M. A. Yahya, Z. Al-Qodah, and C. Z. Ngah, "Agricultural bio-waste materials as potential sustainable precursors used for activated carbon production: A review," *Renewable and Sustainable Energy Reviews*, vol. 46, pp. 218–235, 2015, doi: 10.1016/j.rser.2015.02.051.

[5] G. Crini, "Non-conventional low-cost adsorbents for dye removal: A review," *Bioresource Technology*, vol. 97, no. 9, pp. 1061–1085, 2006, doi: 10.1016/j.biortech.2005.05.001.

[6] K. Singh and S. Arora, "Removal of synthetic textile dyes from wastewaters: A critical review on present treatment technologies," *Critical Reviews in Environmental Science and Technology*, vol. 41, no. 9, pp. 807–878, 2011, doi: 10.1080/10643380903218376.

[7] M. T. Yagub, T. K. Sen, S. Afroze, and H. Ang, "Dye and its removal from aqueous solution by adsorption: A review," *Advances in Colloid and Interface Science*, vol. 209, pp. 172–184, 2014, doi: 10.1016/j.cis.2014.04.002.

[8] V. Gupta and Suhas, "Application of low-cost adsorbents for dye removal – A review," *Journal of Environmental Management*, vol. 90, no. 8, pp. 2313–2342, 2009, doi: 10.1016/j.jenvman.2008.11.017.

[9] M. Rafatullah, O. Sulaiman, R. Hashim, and A. Ahmad, "Adsorption of methylene blue on low-cost adsorbents: A review," *Journal of Hazardous Materials*, vol. 177, nos. 1–3, pp. 70–80, 2010, doi: 10.1016/j.jhazmat.2009.12.047.

[10] P. González-García, "Activated carbon from lignocellulosics precursors: A review of the synthesis methods, characterization techniques and applications," *Renewable and Sustainable Energy Reviews*, vol. 82, pp. 1393–1414, 2018, doi: 10.1016/j.rser.2017.04.117.

[11] H. N. Tran, S. J. You, A. Hosseini-Bandegharaei, and H. P. Chao, "Mistakes and inconsistencies regarding adsorption of contaminants from aqueous solutions: A critical review," *Water Research*, vol. 120, pp. 88–116, 2017, doi: 10.1016/j.watres.2017.04.014.

[12] I. Khan, K. Saeed, I. Zekker, B. Zhang, A. H. Hendi, A. Ahmad, *et al*., "Review on methylene blue: Its properties, uses, toxicity and photodegradation," *Water*, vol. 14, no. 2, Art. no. 242, 2022, doi: 10.3390/w14020242.

[13] N. Littlefield, "Chronic toxicity and carcinogenicity studies of gentian violet in mice," *Fundamental and Applied Toxicology*, vol. 5, no. 5, pp. 902–912, 1985, doi: 10.1016/0272-0590(85)90172-1.

[14] A. Aidoo, N. Gao, R. E. Neft, H. M. Schol, B. S. Hass, T. Y. Minor, *et al*., "Evaluation of the genotoxicity of gentian violet in bacterial and mammalian cell systems," *Teratogenesis, Carcinogenesis, and Mutagenesis*, vol. 10, no. 6, pp. 449–462, 1990, doi: 10.1002/tcm.1770100604.

[15] S. Srivastava, R. Sinha, and D. Roy, "Toxicological effects of malachite green," *Aquatic Toxicology*, vol. 66, no. 3, pp. 319–329, 2004, doi: 10.1016/j.aquatox.2003.09.008.

[16] European Food Safety Authority (EFSA), A. Penninks, K. Baert, S. Levorato, and M. Binaglia, "Dyes in aquaculture and reference points for action," *EFSA Journal*, vol. 15, no. 7, 2017, doi: 10.2903/j.efsa.2017.4920.

[17] K. Kadirvelu, M. Kavipriya, C. Karthika, M. Radhika, N. Vennilamani, and S. Pattabhi, "Utilization of various agricultural wastes for activated carbon preparation and application for the removal of dyes and metal ions from aqueous solutions," *Bioresource Technology*, vol. 87, no. 1, pp. 129–132, 2003, doi: 10.1016/S0960-8524(02)00201-8.

[18] K. Mohanty, J. T. Naidu, B. C. Meikap, and M. N. Biswas, "Removal of crystal violet from wastewater by activated carbons prepared from rice husk," *Industrial & Engineering Chemistry Research*, vol. 45, no. 14, pp. 5165–5171, 2006, doi: 10.1021/ie060257r.

[19] C. Namasivayam and D. Kavitha, "Removal of Congo Red from water by adsorption onto activated carbon prepared from coir pith, an agricultural solid waste," *Dyes and Pigments*, vol. 54, no. 1, pp. 47–58, 2002, doi: 10.1016/S0143-7208(02)00025-6.

[20] S. M. Yakout and M. S. Ali, "Removal of the hazardous crystal violet dye by adsorption on corncob-based and phosphoric acid-activated carbon," *Particulate Science and Technology*, vol. 33, no. 6, pp. 621–625, 2015, doi: 10.1080/02726351.2015.1016642.

[21] C. Namasivayam, N. Muniasamy, K. Gayatri, M. Rani, and K. Ranganathan, "Removal of dyes from aqueous solutions by cellulosic waste orange peel," *Bioresource Technology*, vol. 57, no. 1, pp. 37–43, 1996, doi: 10.1016/0960-8524(96)00044-2.

[22] D. Ramutshatsha-Makhwedzha, A. Mavhungu, M. L. Moropeng, and R. Mbaya, "Activated carbon derived from waste orange and lemon peels for the adsorption of methyl orange and methylene blue dyes from wastewater," *Heliyon*, vol. 8, no. 8, Art. no. e09930, 2022, doi: 10.1016/j.heliyon. 2022.e09930.

[23] M. Abbas, Z. Harrache, and M. Trari, "Mass-transfer processes in the adsorption of crystal violet by activated carbon derived from pomegranate peels: Kinetics and thermodynamic studies," *Journal of Engineered Fibers and Fabrics*, vol. 15, Art. no. 1558925020919847, 2020, doi: 10.1177/1558925020919847.

[24] M. P. Adhikari and J. R. Bhatt, "Remediation of Bagmati River water using activated carbon from Macrotyloma uniflorum (gram horse) seed," *BIBECHANA*, vol. 19, nos. 1–2, pp. 170–183, 2022, doi: 10.3126/bibechana. v19i1-2.46435.

[25] I. D. Mall, V. C. Srivastava, N. K. Agarwal, and I. M. Mishra, "Removal of Congo Red from aqueous solution by bagasse fly ash and activated carbon: Kinetic study and equilibrium isotherm analyses," *Chemosphere*, vol. 61, no. 4, pp. 492–501, 2005, doi: 10.1016/j.chemosphere.2005.03.065.

[26] C. Namasivayam and D. Arasi, "Removal of Congo Red from wastewater by adsorption onto

waste red mud," *Chemosphere*, vol. 34, no. 2, pp. 401–417, 1997, doi: 10.1016/S0045-6535(96)00385-2.

[27] F. Rozada, "Dye adsorption by sewage sludge-based activated carbons in batch and fixed-bed systems," *Bioresource Technology*, vol. 87, no. 3, pp. 221–230, 2003, doi: 10.1016/S0960-8524(02)00243-2.

[28] N. Srivastava, "Temple floral waste management in India," in *Handbook of Solid Waste Management*, pp. 725–756, 2022, doi: 10.1007/978-981-16-4230-2_37.

[29] M. Qiu, L. Liu, Q. Ling, Y. Cai, S. Yu, S. Wang, *et al*., "Biochar for the removal of contaminants from soil and water: A review," *Biochar*, vol. 4, no. 1, Art. no. 19, 2022, doi: 10.1007/s42773-022-00146-1.

[30] M. Molina-Sabio and F. Rodríguez-Reinoso, "Role of chemical activation in the development of carbon porosity," *Colloids and Surfaces A: Physicochemical and Engineering Aspects*, vol. 241, nos. 1–3, pp. 15–25, 2004, doi: 10.1016/j.colsurfa.2004.04.007.

[31] M. Jagtoyen and F. Derbyshire, "Activated carbons from yellow poplar and white oak by H3PO4 activation," *Carbon*, vol. 36, nos. 7–8, pp. 1085–1097, 1998, doi: 10.1016/S0008-6223(98)00082-7.

[32] P. E. Hock and M. A. A. Zaini, "Activated carbons by zinc chloride activation for dye removal – a commentary," *Acta Chimica Slovaca*, vol. 11, no. 2, pp. 99–106, 2018, doi: 10.2478/acs-2018-0015.

[33] H. Zhang, Y. Yan, and L. Yang, "Preparation of activated carbon from sawdust by zinc chloride activation," *Adsorption*, vol. 16, no. 3, pp. 161–166, 2010, doi: 10.1007/s10450-010-9214-5.

[34] W. Tsai, C. Chang, M. Lin, S. Chien, H. Sun, and M. Hsieh, "Adsorption of acid dye onto activated carbons prepared from agricultural waste bagasse by ZnCl2 activation," *Chemosphere*, vol. 45, no. 1, pp. 51–58, 2001, doi: 10.1016/S0045-6535(01)00016-9.

[35] J. Wang and S. Kaskel, "KOH activation of carbon-based materials for energy storage," *Journal of Materials Chemistry*, vol. 22, no. 45, p. 23710, 2012, doi: 10.1039/C2JM34066F.

[36] J. Hou, Y. Liu, S. Wen, W. Li, R. Liao, and L. Wang, "Sorghum-waste-derived high-surface area KOH-activated porous carbon for highly efficient methylene blue and Pb(II) removal," *ACS Omega*, vol. 5, no. 23, pp. 13548–13556, 2020, doi: 10.1021/acsomega.9b04452.

[37] T. Wang, Y. Zhai, Y. Zhu, C. Li, and G. Zeng, "A review of the hydrothermal carbonization of biomass waste for hydrochar formation: Process conditions, fundamentals, and physicochemical properties," *Renewable and Sustainable Energy Reviews*, vol. 90, pp. 223–247, 2018, doi: 10.1016/j.rser.2018.03.071.

[38] R. Foroutan, S. J. Peighambardoust, S. H. Peighambardoust, M. Pateiro, and J. M. Lorenzo, "Adsorption of crystal violet dye using activated carbon of lemon wood and activated carbon/Fe3O4 magnetic nanocomposite from aqueous solutions: A kinetic, equilibrium and thermodynamic study," *Molecules*, vol. 26, no. 8, Art. no. 2241, 2021, doi: 10.3390/molecules26082241.

[39] S. Brunauer, P. H. Emmett, and E. Teller, "Adsorption of gases in multimolecular layers," *Journal of the American Chemical Society*, vol. 60, no. 2, pp. 309–319, 1938, doi: 10.1021/ja01269a023.

[40] M. Thommes, K. Kaneko, A. V. Neimark, J. P. Olivier, F. Rodriguez-Reinoso, J. Rouquerol, *et al*., "Physisorption of gases, with special reference to the evaluation of surface area and pore size distribution (IUPAC Technical Report)," *Pure and Applied Chemistry*, vol. 87, nos. 9–10, pp. 1051–1069, 2015, doi: 10.1515/pac-2014-1117.

[41] M. S. Shafeeyan, W. M. A. W. Daud, A. Houshmand, and A. Shamiri, "A review on surface modification of activated carbon for carbon dioxide adsorption," *Journal of Analytical and Applied Pyrolysis*, vol. 89, no. 2, pp. 143–151, 2010, doi: 10.1016/j.jaap.2010.07.006.

[42] N. Fiol and I. Villaescusa, "Determination of sorbent point zero charge: Usefulness in sorption studies," *Environmental Chemistry Letters*, vol. 7, no. 1, pp. 79–84, 2008, doi: 10.1007/s10311-008-0139-0.

[43] H. Boehm, "Some aspects of the surface chemistry of carbon blacks and other carbons," *Carbon*, vol. 32, no. 5, pp. 759–769, 1994, doi: 10.1016/0008-6223(94)90031-0.

[44] M. Khodaie, N. Ghasemi, B. Moradi, and M. Rahimi, "Removal of methylene blue from wastewater by adsorption onto ZnCl2 activated corn husk carbon equilibrium studies," *Journal of Chemistry*, vol. 2013, no. 1, Art. no. 383985, 2013, doi: 10.1155/2013/383985.

[45] A. T. Ojedokun and O. S. Bello, "Kinetic modeling of liquid-phase adsorption of Congo red dye using guava leaf-based activated carbon," *Applied Water Science*, vol. 7, no. 4, pp. 1965–1977, 2016, doi: 10.1007/s13201-015-0375-y.

[46] K. Foo and B. Hameed, "Insights into the modeling of adsorption isotherm systems," *Chemical Engineering Journal*, vol. 156, no. 1, pp. 2–10, 2010, doi: 10.1016/j.cej.2009.09.013.

[47] M. A. Al-Ghouti and D. A. Da'ana, "Guidelines for the use and interpretation of adsorption isotherm models: A review," *Journal of Hazardous Materials*, vol. 393, Art. no. 122383, 2020, doi: 10.1016/j.jhazmat.2020.122383.

[48] J. Wang and X. Guo, "Adsorption isotherm models: Classification, physical meaning, application and solving method," *Chemosphere*, vol. 258, Art. no. 127279, 2020, doi: 10.1016/j.chemosphere.2020.127279.

[49] I. Langmuir, "The adsorption of gases on plane surfaces of glass, mica and platinum," *Journal of the American Chemical Society*, vol. 40, no. 9, pp. 1361–1403, 1918, doi: 10.1021/ja02242a004.

[50] Q. Hu and Z. Zhang, "Application of Dubinin–Radushkevich isotherm model at the solid/solution interface: A theoretical analysis," *Journal of Molecular Liquids*, vol. 277, pp. 646–648, 2019, doi: 10.1016/j.molliq.2019.01.005.

[51] K. V. Kumar, K. Porkodi, and F. Rocha, "Comparison of various error functions in predicting the optimum isotherm by linear and non-linear regression analysis for the sorption of basic red 9 by activated carbon," *Journal of Hazardous Materials*, vol. 150, no. 1, pp. 158–165, 2008, doi: 10.1016/j.jhazmat.2007.09.020.

[52] H. Yuh-Shan, "Citation review of Lagergren kinetic rate equation on adsorption reactions," *Scientometrics*, vol. 59, no. 1, pp. 171–177, 2004, doi: 10.1023/B: SCIE.0000013305.99473.CF.

[53] Y. Ho and G. McKay, "Pseudo-second order model for sorption processes," *Process Biochemistry*, vol. 34, no. 5, pp. 451–465, 1999, doi: 10.1016/S0032-9592(98)00112-5.

[54] J. P. Simonin, "On the comparison of pseudo-first order and pseudo-second order rate laws in the modeling of adsorption kinetics," *Chemical Engineering Journal*, vol. 300, pp. 254–263, 2016, doi: 10.1016/j.cej.2016.04.079.

[55] C. Aharoni and F. Tompkins, "Kinetics of adsorption and desorption and the Elovich equation," *Advances in Catalysis*, pp. 1–49, 1970, doi: 10.1016/S0360-0564(08)60563-5.

[56] W. J. Weber and J. C. Morris, "Kinetics of adsorption on carbon from solution," *Journal of the Sanitary Engineering Division*, vol. 89, no. 2, pp. 31–59, 1963, doi: 10.1061/JSEDAI.0000430.

[57] E. C. Lima, A. Hosseini-Bandegharaei, J. C. Moreno-Piraján, and I. Anastopoulos, "A critical review of the estimation of the thermodynamic parameters on adsorption equilibria. Wrong use of equilibrium constant in the Van't Hoff equation for calculation of thermodynamic parameters of adsorption," *Journal of Molecular Liquids*, vol. 273, pp. 425–434, 2019, doi: 10.1016/j.molliq.2018.10.048.

[58] J. Marco-Brown, L. Guz, M. Olivelli, B. Schampera, R. Torres Sánchez, G. Curutchet, *et al*., "New insights on crystal violet dye adsorption on montmorillonite: Kinetics and surface complexes studies," *Chemical Engineering Journal*, vol. 333, pp. 495–504, 2018, doi: 10.1016/j.cej.2017.09.172.

[59] O. S. Bello, K. A. Adegoke, O. O. Sarumi, and O. S. Lameed, "Functionalized locust bean pod (Parkia biglobosa) activated carbon for Rhodamine B dye removal," *Heliyon*, vol. 5, no. 8, Art. no. e02323, 2019, doi: 10.1016/j.heliyon. 2019.e02323.

[60] F. Salvador, N. Martin-Sanchez, R. Sanchez-Hernandez, M. J. Sanchez-Montero, and C. Izquierdo, "Regeneration of carbonaceous adsorbents. Part I: Thermal regeneration," *Microporous and Mesoporous Materials*, vol. 202, pp. 259–276, 2015, doi: 10.1016/j.micromeso.2014.02.045.

[61] M. Purkait, A. Maiti, S. DasGupta, and S. De, "Removal of Congo Red using activated carbon and its regeneration," *Journal of Hazardous Materials*, vol. 145, nos. 1–2, pp. 287–295, 2007, doi: 10.1016/j.jhazmat.2006.11.021.

[62] M. León, J. Silva, S. Carrasco, and N. Barrientos, "Design, cost estimation and sensitivity analysis

for a production process of activated carbon from waste nutshells by physical activation," *Processes*, vol. 8, no. 8, Art. no. 945, 2020, doi: 10.3390/pr8080945.

[63] C. Qin, Y. Chen, and J. M. Gao, "Manufacture and characterization of activated carbon from marigold straw (Tagetes erecta L) by H3PO4 chemical activation," *Materials Letters*, vol. 135, pp. 123–126, 2014, doi: 10.1016/j.matlet.2014.07.151.

[64] A. Ahmed, M. Rafat, and S. Ahmed, "Activated carbon derived from custard apple shell for efficient supercapacitor," *Advances in Natural Sciences: Nanoscience and Nanotechnology*, vol. 11, no. 3, Art. no. 035013, 2020, doi: 10.1088/2043-6254/aba1dc.

[65] K. Kapoor, M. Bala, P. Choudhary, D. Mridula, and R. Singh, "Development of method for detection of Rhodamine B dye in chilli powder (Capsicum annuum L.)," *Asian Journal of Dairy and Food Research*, 2022, doi: 10.18805/ajdfr. DR-1733.

[66] K. Patidar and M. Vashishtha, "Activated carbon from mustard stalk biomass: Synthesis, characterization and application in wastewater treatment," *Journal of the Serbian Chemical Society*, vol. 86, no. 4, pp. 429–444, 2021, doi: 10.2298/JSC201103010P.

[67] A. Medhat, H. H. El-Maghrabi, A. Abdelghany, N. M. Abdel Menem, P. Raynaud, Y. M. Moustafa, *et al*., "Efficiently activated carbons from corn cob for methylene blue adsorption," *Applied Surface Science Advances*, vol. 3, Art. no. 100037, 2021, doi: 10.1016/j.apsadv.2020.100037.

[68] L. Brahmi, F. Kaouah, S. Boumaza, and M. Trari, "Response surface methodology for the optimization of acid dye adsorption onto activated carbon prepared from wild date stones," *Applied Water Science*, vol. 9, no. 8, Art. no. 171, 2019, doi: 10.1007/s13201-019-1053-2.

[69] P. P. Kyi, J. O. Quansah, C. G. Lee, J. K. Moon, and S. J. Park, "The removal of crystal violet from textile wastewater using palm kernel shell-derived biochar," *Applied Sciences*, vol. 10, no. 7, Art. no. 2251, 2020, doi: 10.3390/app10072251.

[70] E. Akar, A. Altinişik, and Y. Seki, "Using of activated carbon produced from spent tea leaves for the removal of malachite green from aqueous solution," *Ecological Engineering*, vol. 52, pp. 19–27, 2013, doi: 10.1016/j.ecoleng.2012.12.032.

[71] J. M. Jabar, M. A. Adebayo, I. A. Owokotomo, Y. A. Odusote, and M. Yılmaz, "Synthesis of high surface area mesoporous ZnCl2–activated cocoa (Theobroma cacao L) leaves biochar derived via pyrolysis for crystal violet dye removal," *Heliyon*, vol. 8, no. 10, Art. no. e10873, 2022, doi: 10.1016/j.heliyon. 2022.e10873.

[72] B. Gayani, A. C. Perera, and N. Kottegoda, "Thermodynamic, equilibrium and kinetic studies of adsorption of Rhodamine B onto activated bamboo carbon," *Desalination and Water Treatment*, vol. 67, pp. 271–283, 2017, doi: 10.5004/dwt.2017.20386.

[73] O. Üner, Ü. Geçgel, H. Kolancilar, and Y. Bayrak, "Adsorptive removal of Rhodamine B with activated carbon obtained from okra wastes," *Chemical Engineering Communications*, vol. 204, no. 7, pp. 772–783, 2017, doi: 10.1080/00986445.2017.1319361.

[74] R. Gong, J. Ye, W. Dai, X. Yan, J. Hu, X. Hu, *et al*., "Adsorptive removal of methyl orange and methylene blue from aqueous solution with finger-citron-residue-based activated carbon," *Industrial & Engineering Chemistry Research*, vol. 52, no. 39, pp. 14297–14303, 2013, doi: 10.1021/ie402138w.

[75] K. Mahmoudi, N. Hamdi, A. Kriaa, and E. Srasra, "Adsorption of methyl orange using activated carbon prepared from lignin by ZnCl2 treatment," *Russian Journal of Physical Chemistry A*, vol. 86, no. 8, pp. 1294–1300, 2012, doi: 10.1134/S0036024412060180.